

Toxicity of Sodium Fluoride in Liver of Albino Rat and the Beneficial Effect of Calcium in Reversing Fluoride Toxicity: Histological, Ultrastructural and Immunohistochemical Studies

Amal Seliman Sewelam

Department of Anatomy and Embryology, Faculty of Medicine, Zagazig University

E-mail: ali121212121213@yahoo.com, Phone: 00201155789552

ABSTRACT

Background: fluoride (F) is an essential element for human being from health point of view. Its intake in high doses caused toxic effects on various organs. The liver is a target organ for F toxicity. Using natural supplements is a modern approach in treatment.

Aim of the Study: this study aimed to investigate the effect of sodium fluoride (NaF) on liver tissue in adult male albino rats and also to determine whether calcium(Ca) co-treatment has an ameliorative role in reversing F toxicity or not.

Material and Methods: eighteen adult albino male rats were categorized into three groups (each of six animals): Group I (Control): were given distilled water and fed balanced diet, Group II (NaF treated): were given NaF at a dose of 30 mg /kg/day and Group III (NaF and Ca treated): were received NaF (similar previous dose) and 20 mg /kg/day calcium chloride (CaCl). After six weeks, under anesthesia, the livers were rapidly delivered, dissected out carefully, prepared and examined by light and electron microscopy, biochemical, immunohistochemical, morphometric studies.

Results: the results showed that F induced severe histopathological changes in the liver tissue, significantly increased apoptosis and hepatic marker enzymes as compared to the control group. The histopathological changes induced by NaF included hepatocytic vacuolization, pyknosis and necrosis, vascular dilatation and congestion, Kupffer cell proliferation and periportal inflammatory cell infiltration. The ultra structural changes of hepatocytes included nuclear disorganization (Being heterochromatic, pyknotic nuclei or disintegrated chromatin), vague mitochondria ridges, fragmentation of the rough endoplasmic reticulum, dispersed ribosomes, disruption of hepatocytes microvilli, ill defined space of Disse, Kupffer cell activation and bile canalicular dilatation. Co-treatment with Ca failed to improve liver tissue damages induced by NaF treatment.

Conclusion: results of this study suggested that NaF treatment caused severe damages to liver tissue. Ca co-administration failed to reset NaF induced hepatotoxicity.

Keywords: fluoride, liver, calcium, apoptosis, Caspase-3.

INTRODUCTION

Fluoride (F) is very widely distributed in the natural environment and is extensively used among industry, agriculture as well as medicine⁽¹⁾. It is an essential trace element for human body and is a normal constituent of soft tissues, body fluids, teeth and bones⁽²⁾. F sources are either natural or artificial and include fluoridated foodstuffs, insecticides, ground water, toothpaste, drugs, vapors released from industries using fluoride containing compounds and dentifrices⁽³⁾. Moderate levels of F intake promote bone development and are useful for caries prevention. However ingestion or inhalation of high F doses causes adverse effects on human and animal health^(4,5). F toxicity targets not only the bone and teeth⁽⁶⁾, but also soft tissues including kidney⁽⁷⁾, brain⁽⁸⁾ and blood⁽⁹⁾. It has a toxicity on cells, genes and immune system and can induce lesions in the peripheral blood, kidney, spleen and intestine⁽¹⁰⁾ and in the mouse spleen and kidney^(11,12,13). Being very active organ, the liver is involved in metabolism and elimination of toxic substances from the body. It's

histological and biochemical parameters are very important to detect toxicity of chemicals. Subsequently, the liver is specifically liable to F toxicity⁽¹⁴⁾. Serum ALT, AST, ALK are known to be important markers to investigate the health of an animal species. ALT and AST are present in the mitochondria and cytoplasm respectively mainly in the liver. They are also located in striated and cardiac muscles and have a vital role in protein metabolism. High serum levels of these enzymes have been used as an indicator of tissue damage⁽¹⁵⁾. Previous studies have suggested that excessive F intake can induce oxidative stress and subsequently apoptosis^(2,16,10). Caspases are present in cells as inactive zymogens and undergo a series of catalytic activation at the beginning of apoptosis⁽¹⁷⁾. Therefore, the activity of-caspase-3 could be checked to detect apoptosis. Marked improvement of F cytotoxicity when co-administered with a combination of carnosin, vitamin E and methionine has been shown⁽¹⁸⁾ and when given in combination with each of quercetin, black tea extract, gallic acids and ferulic^(19,20,14,21)

respectively. On the other hand, published reports on the role of Ca against F toxicity were little. Ca is an abundant mineral in the body and is available in several foods, dietary supplements and medicines like antacids⁽²²⁾. Significant recovery from F toxicity was revealed when calcium phosphate was co-administered with ascorbic acid and given to NaF-treated mice⁽²³⁾. However, a study has suggested that F induced cellular changes were associated with altered Ca homeostasis⁽²⁴⁾. This study aimed to investigate the effects of F on liver of adult male albino rat using histological, ultrastructural, biochemical and immunohistochemical methods and also to investigate if Ca has a possible role to alleviate F induced hepatotoxicity or not.

MATERIAL and METHODS

Chemicals: NaF and CaCl and all other chemicals were obtained from Sigma Chemical Company.

Animals and treatment: this study was carried out on 18 adult male albino rats (2 months old and 250-300 g weight) obtained from the Farm of Laboratory Animals, Faculty of Veterinary Medicine, Zagazig University. The rats were housed at a constant temperature of 21 ± 2 °C, fed standard diets with water available *ad libitum* and kept under a 12-h light / dark cycle (lights on at 8:00 am). They were randomly categorized into 3 groups, 6 animals for each, treated orally by gastric feeding tube as described below for 6 consecutive weeks. **Group I (Control group)** received distilled water, **Group II (NaF treated group)** received drinking water with NaF dosed 30 mg /kg/day and **Group III (NaF and Ca treated group)** received NaF (the same previous dose) and CaCl dosed 20 mg /kg/day at the same time. Dose selection of NaF and CaCl was based on previous established studies^(25, 26). At the end of the experiment, the rats were randomly selected and anaesthetized, their abdomens were opened and the livers were rapidly extracted, dissected out carefully and processed for light and electron microscope examination.

Biochemical assays

Samples of blood obtained by cardiac puncture were collected into heparinized tubes. The serum was used to evaluate liver function by estimation of levels of activities of aspartate aminotransferase (AST), alanine aminotransferase (ALT) and alkaline phosphatase (ALP) enzymes by the methods of **Reitman and Frankel**⁽²⁷⁾.

I-Preparation for light microscopy: (Suvarna *et al.*)⁽²⁸⁾.

The liver tissues of animals from each experimental group were fixed in 10% neutral formalin for 48–72

h. The tissues were trimmed and processed for routine histological examination. Then, they were embedded in paraffin wax and 4–5 μ sections were cut. Hematoxylin and eosin staining was used for all tissue sections. Tissue slides were examined under a light microscope in the Department of Oral Pathology, Faculty of Dental Medicine, Cairo University.

II-Preparation for Transmission electron microscopy: (Glauert and Lewis)⁽²⁹⁾

Samples from fresh liver specimens obtained for transmission electric microscope (TEM) from animals of each experimental group were immediately fixed in 1% osmic acid and dehydrated in graded alcohol series. Resin sections of 50-nm were cut on resin microtome and dyed using uranyl acetate and lead citrate for electron microscopic examination in Departments of Histology, Faculty of Medicine, Zagazig and Tanta Universities.

III-Immunohistochemical technique:

Immunohistochemical reactions were performed on sections of liver tissue obtained from all the experimental groups using Caspase 3 antibody to identify caspase-positive apoptotic cells, sections of liver tissue were stained with rabbit-anti-cleaved caspase-3 antibodies (From Cell Signaling Technology, Inc, Beverly, USA; Cat. No. 9661 and 9507) delivered from DAKO life trade Egypt. Routine immunohistochemical methods specifically as described by **Unger *et al.***⁽³⁰⁾ were established. 5 μ paraffin sections were heated in a microwave oven (25 min at 720 W) for antigen retrieval and then, incubated with the anti-caspase antibodies (1:50 dilution) overnight at 4°C. This was followed by incubation with biotinylated goat-anti-rabbit-IgG secondary antibodies (1:200 dilution; Biospa, Milano, Italy) and streptavidin/alkaline phosphatase complex (1:200 dilution; Biospa). Hematoxylin was used as a counter stain for nuclei. In routine histological sections, the immunohistochemical staining resulted in brown yellow reaction product in antigen-containing cells, whereas the background stained blue. Areas positive for a particular color of dye were selected and area percent was calculated by using software.

IV-Image analysis and morphometric studies: area percent

The image analyser computer system was used by using the software Leica Quin 500 at Oral Pathology Department, Faculty of Dental Medicine, Cairo University. It measures the area percent of the caspase-3 protein expression in liver tissue of rats / unit area. (Unit area = microscopic field) in a standard measuring frame using a magnification x400 by light microscopy transferred to the monitor's screen. These areas were masked by a

green color using the computer system (**Figure 1**). Area percent values for each experimental group were obtained from 5 different fields from different slides. Values were presented as mean and standard deviation.

V- Statistical analysis

Statistical analysis was performed by using Statistical Package of Social Science (SPSS), software version 22.0 (SPSS Inc., 2013). Data were

normally distributed (Parametric) and so expressed as mean \pm SD. Statistical differences among the experimental groups were determined using one-way ANOVA. Multiple comparisons between groups were performed using Post hoc Tukey's test. Differences at $p < 0.05$ or less were considered significant. All statistical calculations were carried out by using Graphpad Prism, Version 5.0 Software (Graphpad Software, San Diego, CA, USA).

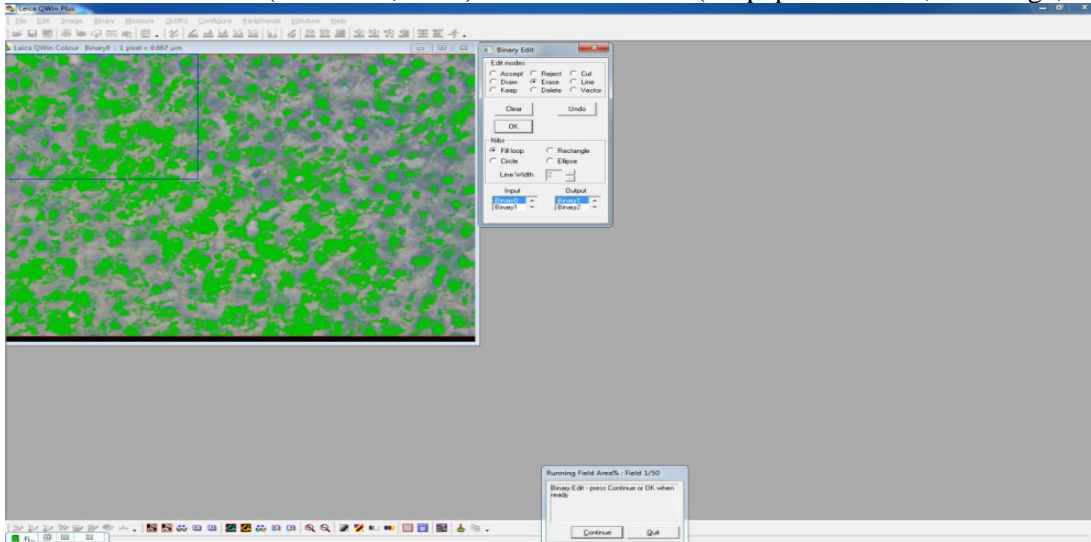


Fig. 1: a photomicrograph of a copy of display monitor's screen of the image analyzer showing the method of measurement of area % of the immunohistochemical localization of caspase 3 in tissues / unit area (masked by green marker). (IHC of caspase 3 x400)

RESULTS

A- Histological results: (Light and electron microscopes examination):

Light microscopy:

The liver of control rats (**Group I**) showed normal structure of the hepatic lobules, each was formed of hepatic cords separated by blood sinusoids lined with Kupffer cells and radiating from the central vein lined with thin endothelial cells. The hepatic cords exhibited polyhedral hepatocytes with central rounded vesicular nuclei and acidophilic cytoplasm. Some hepatocytes were binucleated (**Figure 2**). A portal area containing portal vein and bile duct was revealed (**Figure 3**). Treatment with NaF (**Group II**) caused severe liver damage with disrupted architecture of hepatic lobules and dilated central veins (**Figure 4**). The dilated central vein contained hemolysed blood cells with necrosis of its endothelial lining. The blood sinusoids appeared dilated, congested with increased Kupffer cells (**Figure 5**). The hepatocytes showed marked degenerative changes manifested by cytoplasmic vacuolization and pyknotic nuclei. Multiple areas of necrosis were observed denoting complete cell lysis (**Figure 6**).

The portal vein was markedly dilated, thick walled, congested and contained hemolysed blood

cells. Also, extensive periportal inflammatory cell infiltration was observed. The bile ducts appeared dilated and the hepatic artery had a thick wall (**Figure 7**).

In NaF and Ca treated group (**Group III**), as compared to NaF treated group, there were extensive liver tissue damages manifested by markedly distorted cytoarchitecture, centrilobular and focal necrosis, markedly dilated central vein and severe congestion (**Figure 8**). Most hepatocytes showed extensive vacuolization with darkly stained nuclei. Others showed complete lysis leaving severely congested dilated sinusoidal spaces. Clumps of pyknotic nuclei were also observed (**Figure 9**). Other hepatocytes appeared shrunken with dilated congested distorted sinusoidal spaces and Kupffer cell hyperplasia (**Figure 10**). The portal vein was extensively dilated and congested. Markedly thick walled hepatic artery and bile ducts dilatation and proliferation were well observed (**Figure 11**).

Transmission electron microscopy

In the control group (**Group I**), the hepatocytes exhibited rounded euchromatic nuclei with regular nuclear envelopes. The cytoplasm showed abundant polymorphic mitochondria with well developed transverse cristae and electron dense matrix, well developed endoplasmic reticulum profiles exhibiting regular orientation around the nucleus and clusters of ribosome (**Figure 12**). Tight junctions and bile ducts containing microvilli lying in between two adjacent hepatocytes were well demonstrated (**Figure 13**). Kupffer cells were seen lining sinusoids and exhibited thin filipodia, cytoplasmic phagolysosomes with clear Disse spaces between them and hepatocytic microvilli (**Figure 14**).

In NaF-treated group (**Group II**), hepatocytes were severely degenerated and showed shrinkage, cytoplasmic vacuolization, hazy organelles and deformed nuclei which were either heterochromatic (exhibiting clumping and margination of chromatin) or pyknotic (shrunken and hyperchromatic) or disintegrated (**Figure 15**). Some hepatocytes appeared apoptotic (showing detachment, shrinkage with decreased cytoplasmic density and pyknotic nuclei) (**Figure 16**). Most hepatocyte vacuoles were large compressing cytoplasmic organelles and closely opposed to mitochondrion with unclear ridges. Fragmented and decreased endoplasmic reticulum, dispersed ribosome (**Figure 17**) and areas of decreased cytoplasmic density denoting lysis of cytoplasm and organelles were well demonstrated. Destructed hepatocyte microvilli projecting into ill defined space of Disse with active Kupffer cells characterized by numerous phagolysosomes were

seen lining dilated congested hepatic sinusoids (**Figure 18**). Disrupted hepatocyte cell membrane and disintegrated nuclear membrane were also noticed (**Figure 19**). The bile ducts between two adjacent hepatocytes exhibited dilatation and the projecting microvilli were fragmented and decreased in number with distorted junctions between cells (**Figure 20**).

In NaF and Ca treated group (**Group III**), the ultra structural results of this work showed more extensive toxic changes in liver when compared to NaF treated group. The most distinct damages observed were hepatocellular necrosis manifested by disrupted plasma membranes and fragments of degenerated organelles were dispersed in the extracellular spaces. Most hepatocytic mitochondria appeared spherical in shape denoting swelling and others were disintegrated. Heterochromatic nuclei with prominent nucleoli were also observed (**Figure 21**). Many hepatocytes were apoptotic and showed shrinkage with pyknotic nuclei (deformed hyperchromatic with defected nuclear membranes), high electron density of cytoplasm, extensive cytoplasmic vacuolization and fragmented hepatocyte microvilli (**Figure 22**). Extensively dilated bile ducts with destructed microvilli were manifested (**Figure 23**). Markedly dilated and congested hepatic sinusoids lined with very active Kupffer cells characterized by filipodia and huge number of phagolysosomes were well recognized. The hepatocytes microvilli were destructed and the space of Disse was ill defined (**Figure 24**).

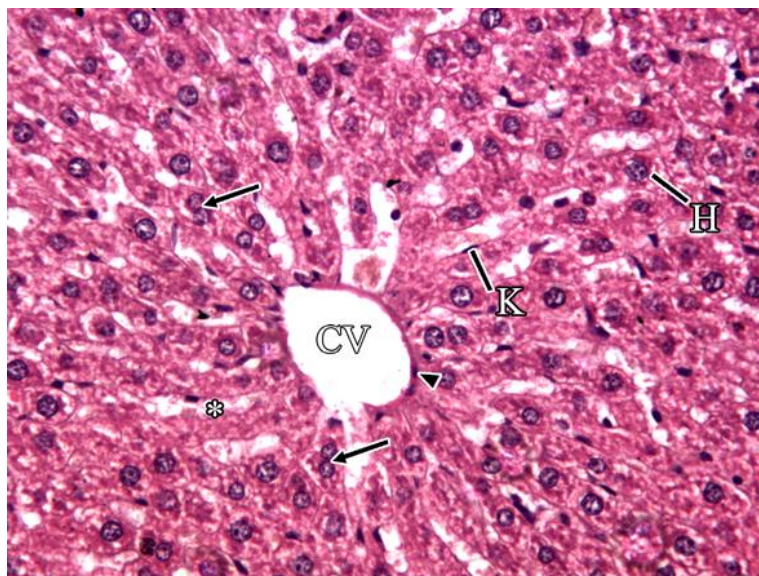


Fig. 2: a photomicrograph of a liver section of a control rat (**Group I**) showing cords of hepatocytes (H) radiating from central vein (CV) which is lined by thin endothelial cells (arrowhead). These cords are

separated by sinusoids (*) lined by Kupffer cells (K). Some binucleated hepatocytes are noticed (arrows). (H&E x400)

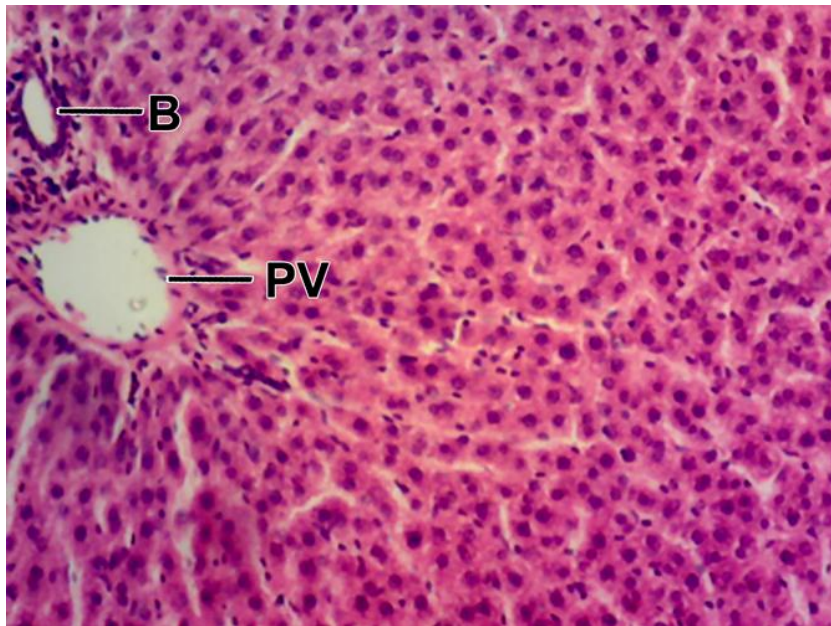


Fig. 3: a photomicrograph of a liver section of a control rat (**Group I**) showing the portal area containing the portal vein (PV) and the bile duct (B). (H&E x200)

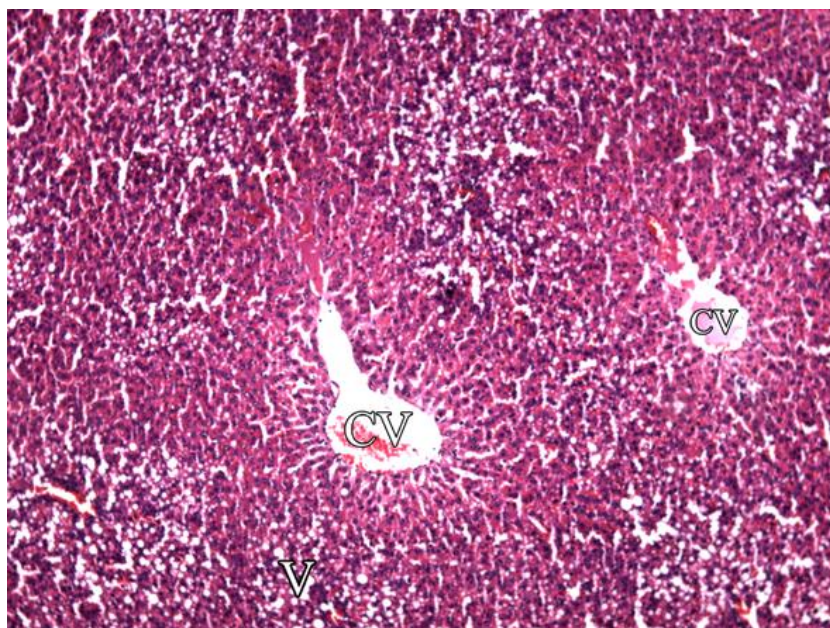


Fig. 4: a photomicrograph of a section of NaF treated rat liver (**Group II**) showing disrupted architecture of the hepatic lobules, extensive vacuolization (V) and markedly dilated central veins (CV). (H&E x100)

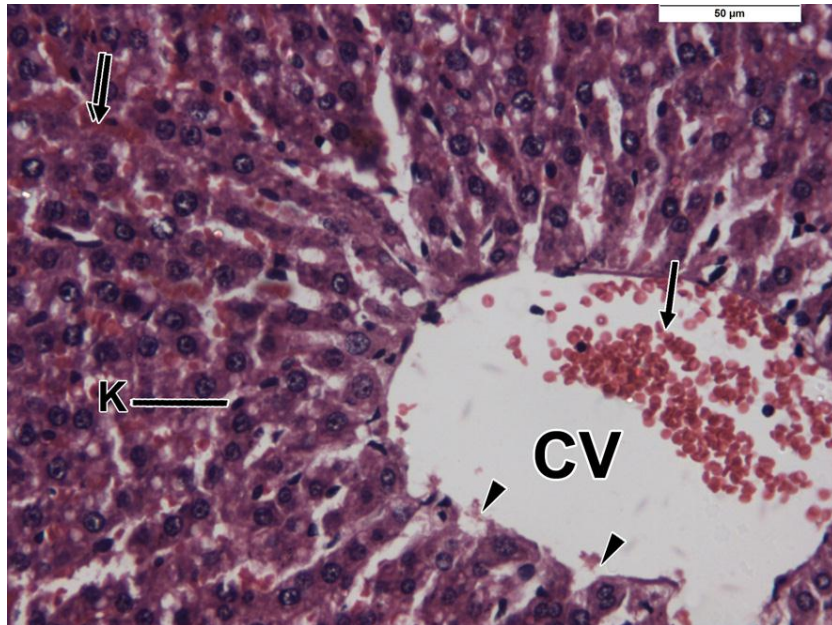


Fig. 5: a higher magnification of figure 4 showing the markedly dilated central vein (CV) containing hemolysed blood cells (arrow) with necrosis of its endothelial lining (arrowheads). Congested dilated blood sinusoids (double arrows) with increased Kupffer cells (K) are well recognized. (H&Ex400)

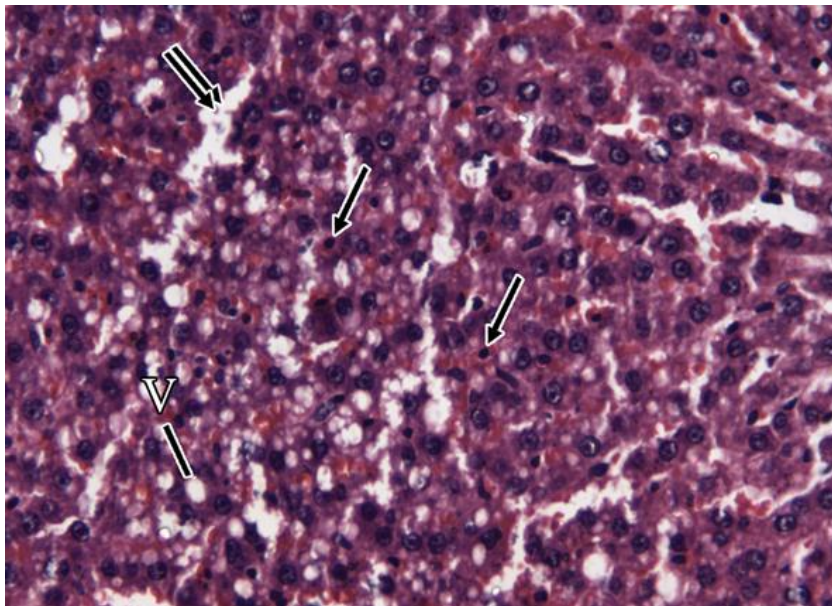


Fig. 6: a higher magnification of figure 4 showing cytoplasmic vacuolization (V) and pyknotic nuclei (arrows) of hepatocytes. Numerous necrotic areas (double arrows) are observed. (H&E x400)

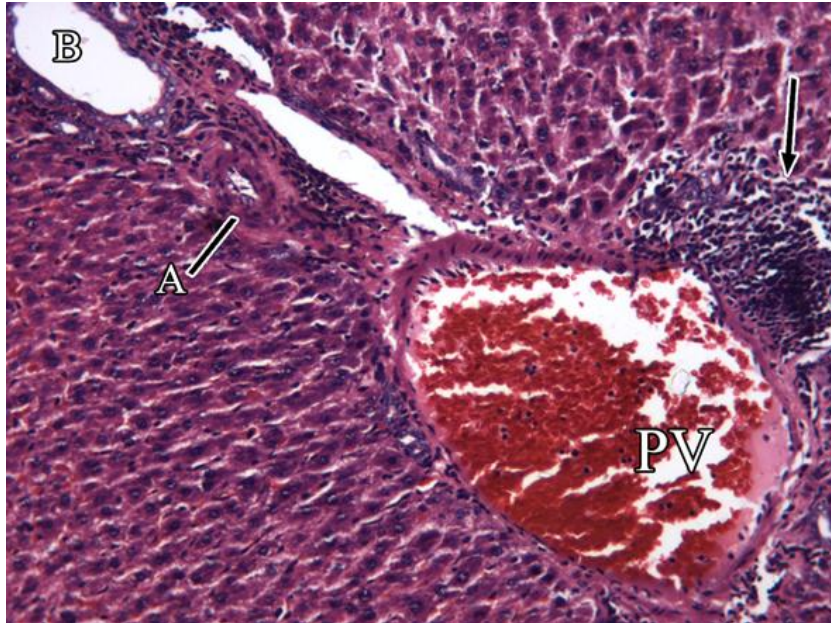


Fig.7 : a photomicrograph of a section of NaF treated rat liver (**Group II**) showing markedly dilated, congested thick walled portal vein containing hemolysed blood cells (PV), extensive periportal infiltration with inflammatory cells (arrow), dilated bile ducts (B) and thick walled hepatic artery (A). (H&E x200)

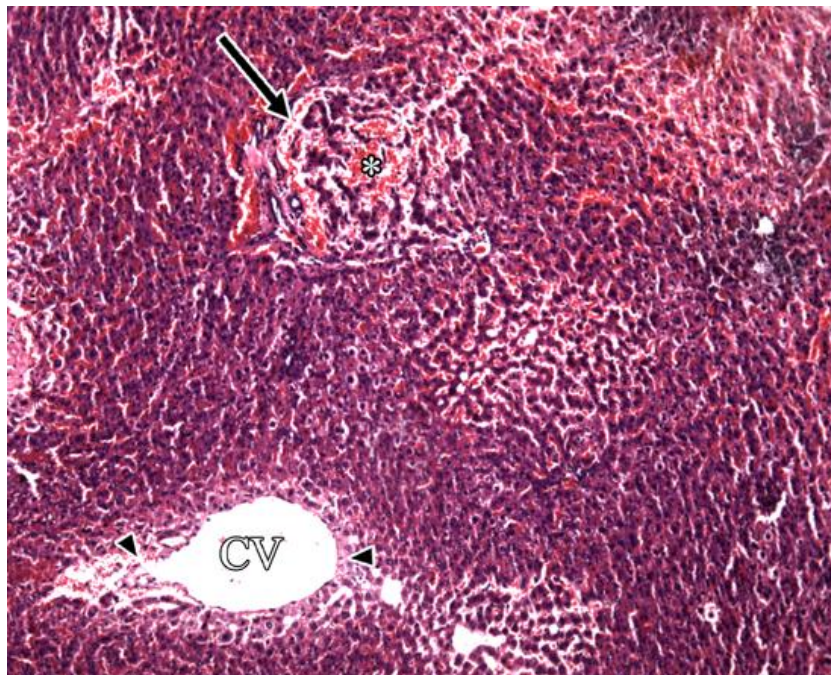


Fig.8: a photomicrograph of a section of NaF and Ca treated rat liver (**Group III**) showing severely distorted hepatic structure , centrilobular (arrowhead) and focal necrosis(arrows), markedly dilated central vein (CV) and severe congestion (*). (H&E x100)

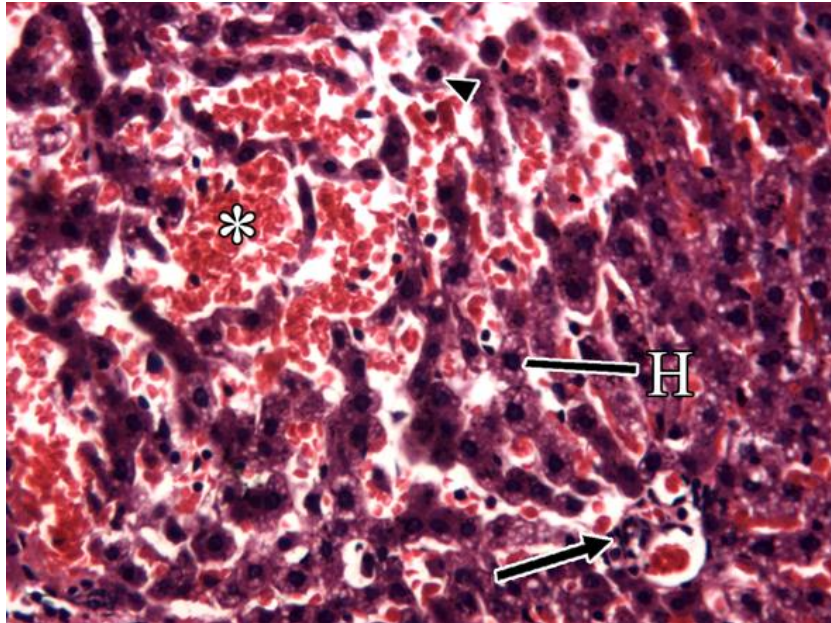


Fig. 9: a higher magnification of the previous figure showing extensively vacuolated hepatocytes (H) with darkly stained nuclei (arrowhead). Other hepatocytes show complete lysis leaving severely congested and dilated sinusoidal spaces (*). Clumps of pyknotic nuclei are observed (arrow). (H&E x400)

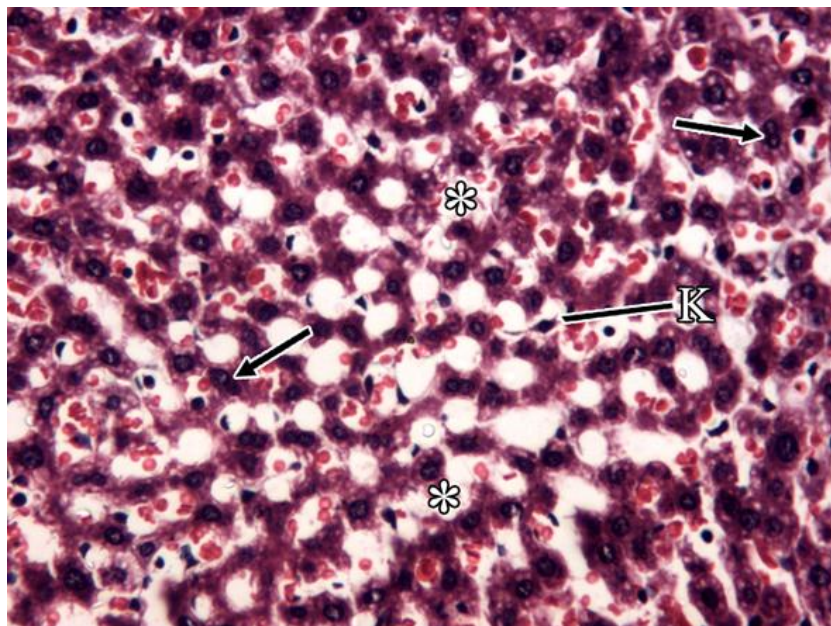


Fig. 10: a photomicrograph of a section from NaF and ca treated rat liver (**Group III**) showing shrunken hepatocytes with dilated, congested and distorted sinusoids(*) and Kupffer cell hyperplasia (K). (H&E x400)

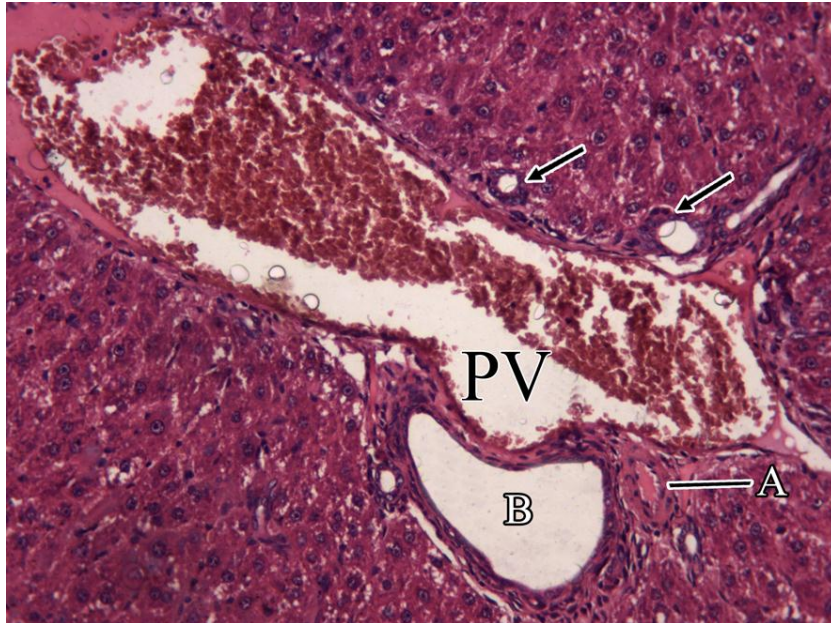


Fig.11: a photomicrograph of a section from NaF and ca treated rat liver (**Group III**) showing highly dilated congested portal vein (PV), markedly thick walled hepatic artery (A) and bile ducts dilatation (B) and proliferation(arrows). (H&E x200)

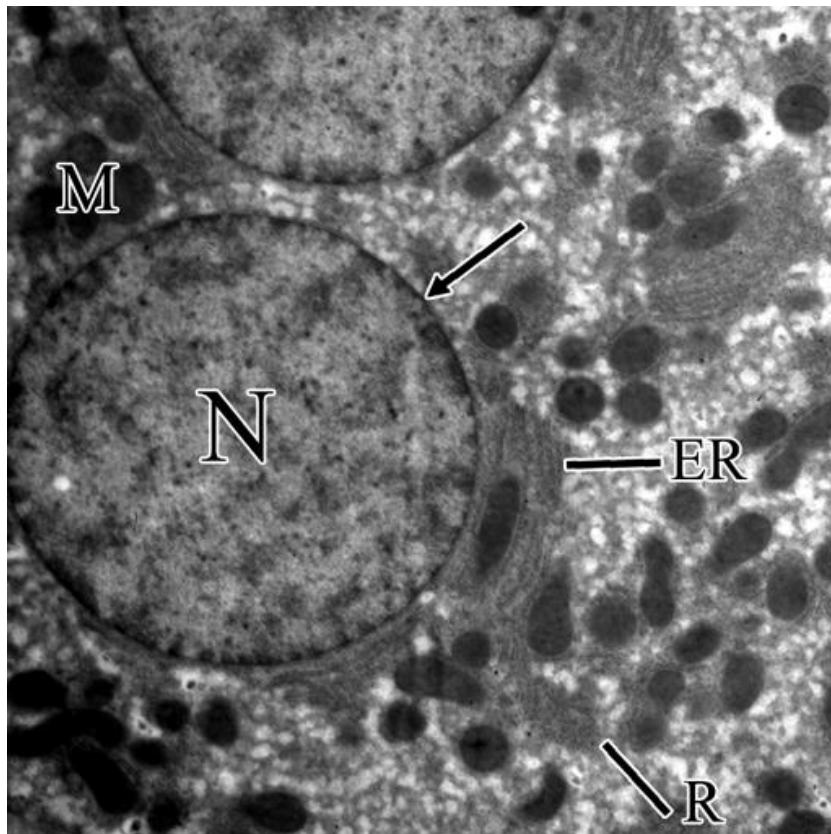


Fig. 12: an electron micrograph of liver section of control rat (**Group I**) showing the hepatocyte exhibiting rounded euchromatic nuclei (N) with regular nuclear envelopes (arrow), polymorphic mitochondria (M), endoplasmic reticulum (ER) and clusters of ribosome (R). (x 8000)

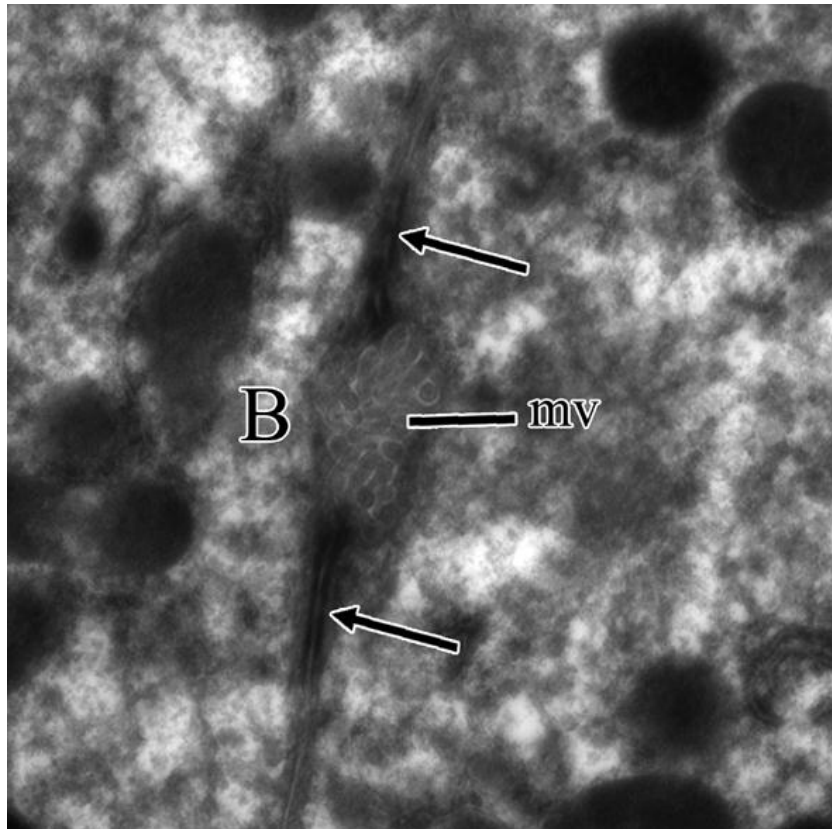


Fig. 13: an electron micrograph of liver section of control rat (Group I) showing tight junctions (arrows) and bile ducts(B) containing microvilli (mv) lying between two adjacent hepatocytes (x 40,000)

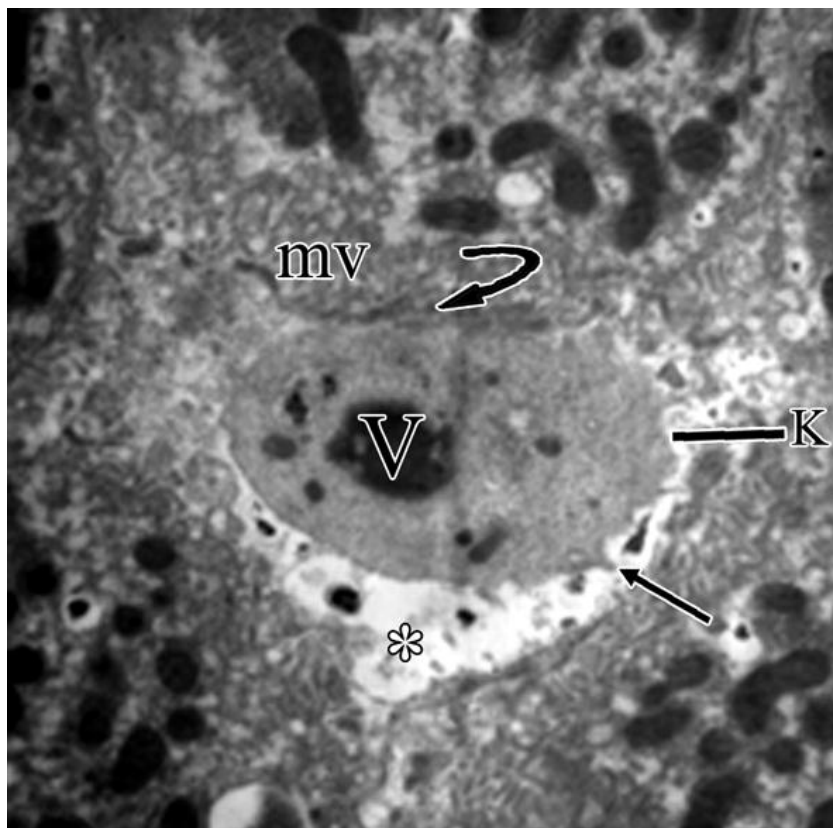


Fig.14: an electron micrograph of liver section of control animal (Group I) showing the Kupffer cell (K) lining hepatic sinusoid (*) and exhibiting thin filipodia (arrow), cytoplasmic phagolysosomes (V) and clear Disse space (curved arrow) between it and hepatocytic microvilli (mv). (x 8000)

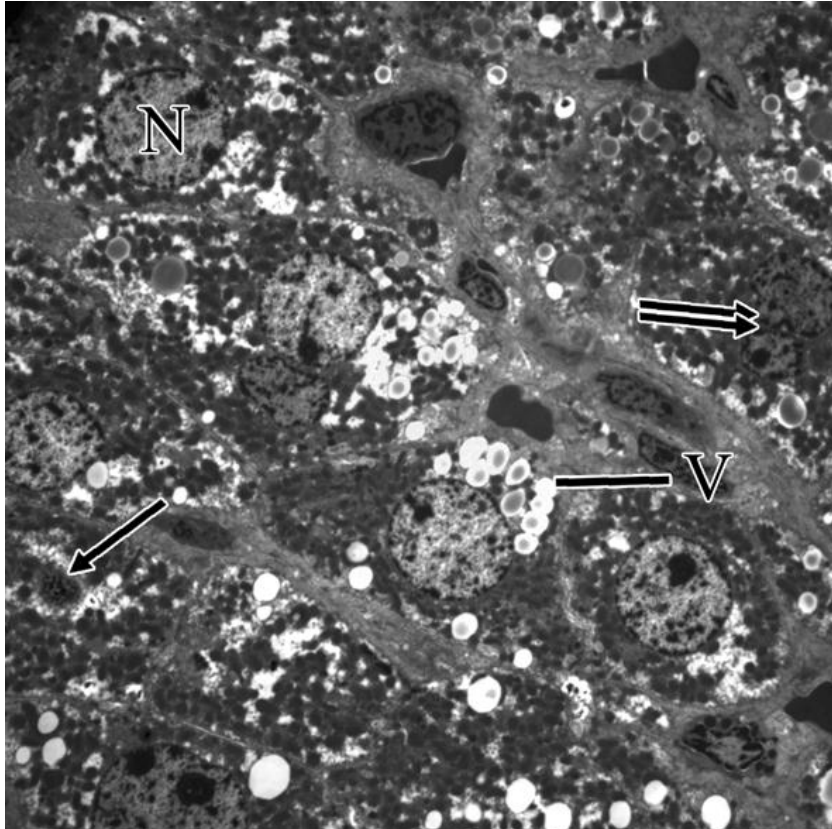


Fig.15: an electron micrograph of a section of NaF-treated rat liver (**Group II**) showing shrunken hepatocytes with heterochromatic (N), pyknotic (double arrows) or disintegrated (arrow) nuclei and marked cytoplasmic vacuolization (V). (x 2500)

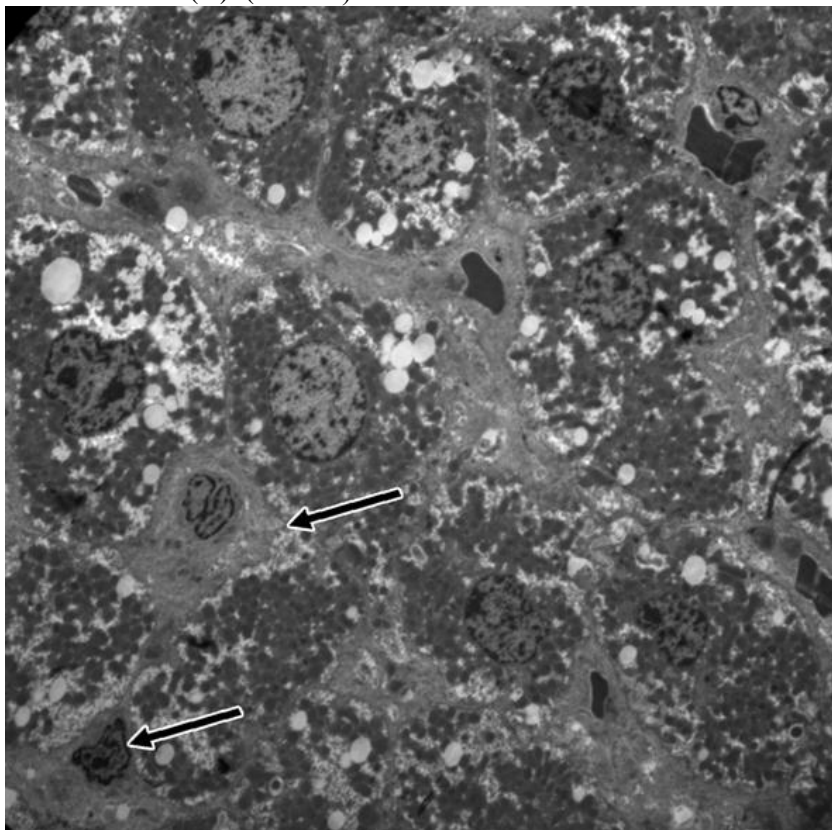


Fig. 16: an electron micrograph of a section of NaF-treated rat liver (**Group II**) showing apoptotic hepatocytes (arrows). (x 2500)

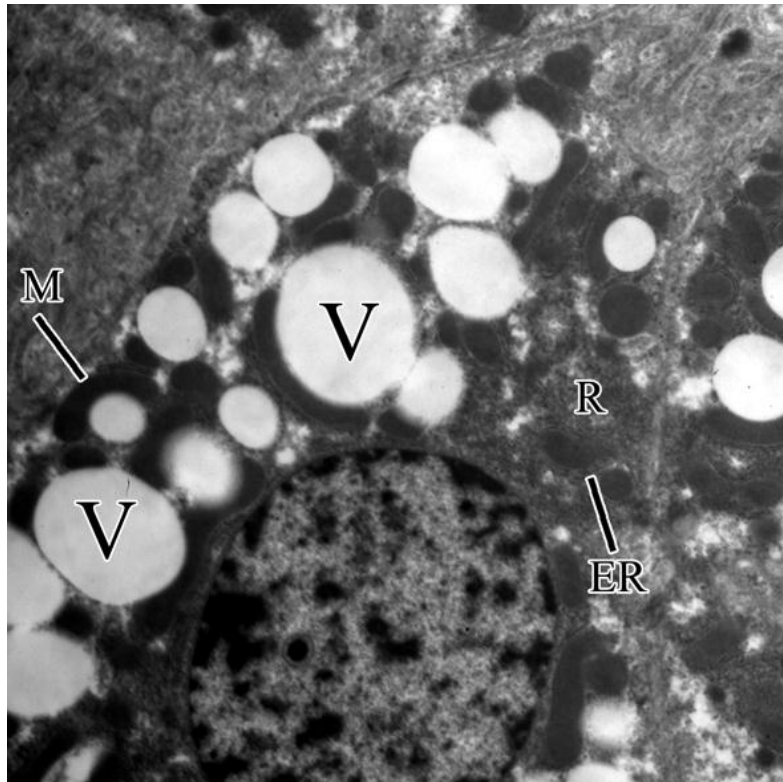


Fig.17: an electron micrograph of a section of NaF-treated rat liver (**Group II**) showing large hepatocytic vacuoles (V) closely opposed to hazy mitochondrion (M), fragmented and decreased endoplasmic reticulum (ER) and dispersed ribosomes (R). (x8000)

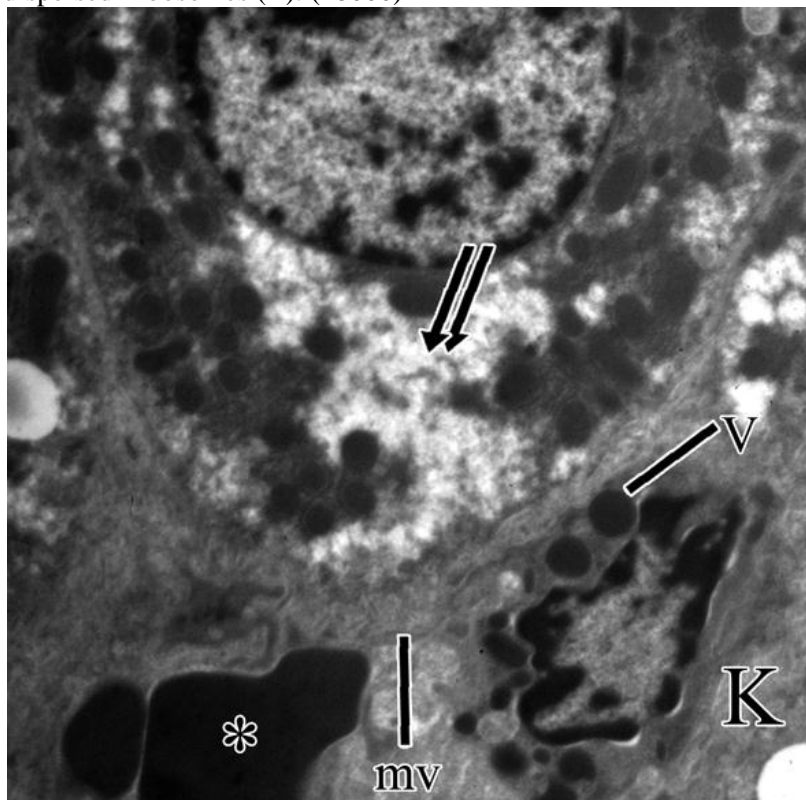


Fig. 18: an electron micrograph of a section of NaF-treated rat liver (**group II**) showing decreased cytoplasmic density of hepatocyte (double arrows) with fragmented microvilli (mv). Active Kupffer cell (K) containing numerous phagolysosomes (V) is seen lining dilated congested sinusoid (*). (x8000)

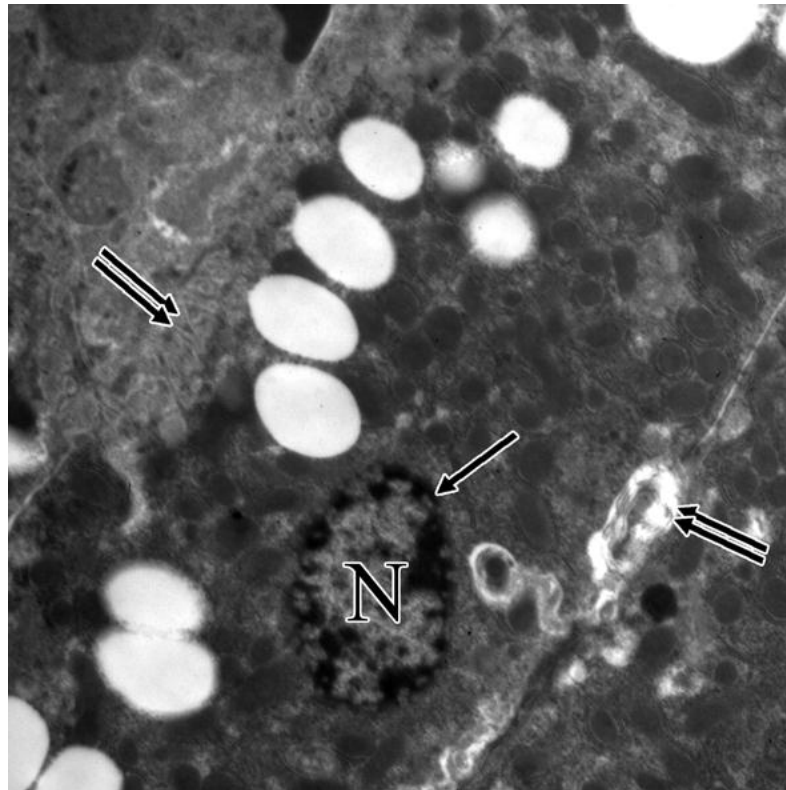


Fig. 19: an electron micrograph of a liver section of NaF-treated rat (Group II) pyknotic nucleus (N) with disintegrated nuclear membrane (arrow) and disrupted hepatocyte cell membrane (double arrows). (x8000)

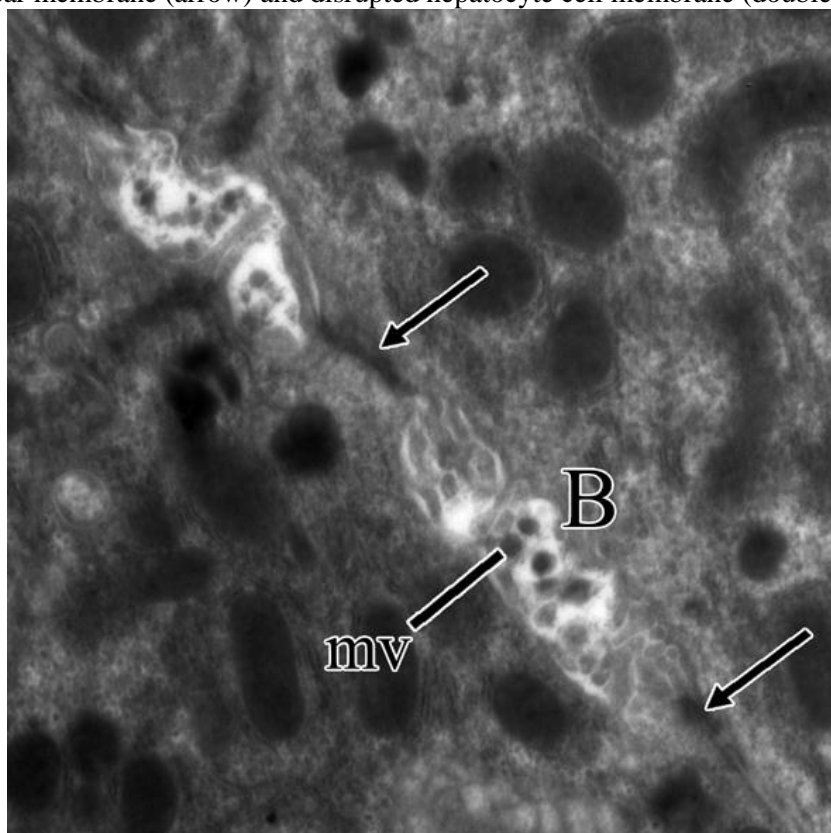


Fig. 20: an electron micrograph of a liver section of NaF-treated rat (Group II) showing two adjacent hepatocytes with dilated bile canaliculus (B), markedly fragmented microvilli (mv) and distorted junctions (arrows). (x 20000)

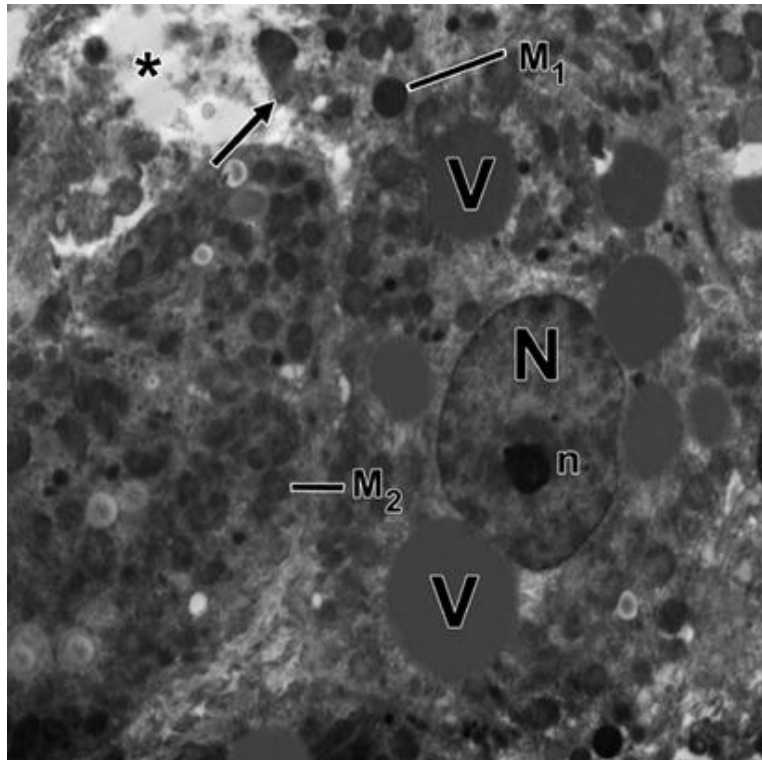


Fig. 21: an electron micrograph of a section of NaF and Ca treated rat liver (**Group III**) showing hepatocytic necrosis manifested by plasma membrane disruption(arrow) and dispersion of fragments of degenerated organelles in the extracellular space (*). Heterochromatic nucleus (N) with prominent nucleolus(n),swollen (M1), disintegrated mitochondria (M2) and multiple vacuoles (V)are also seen. (x 5000)

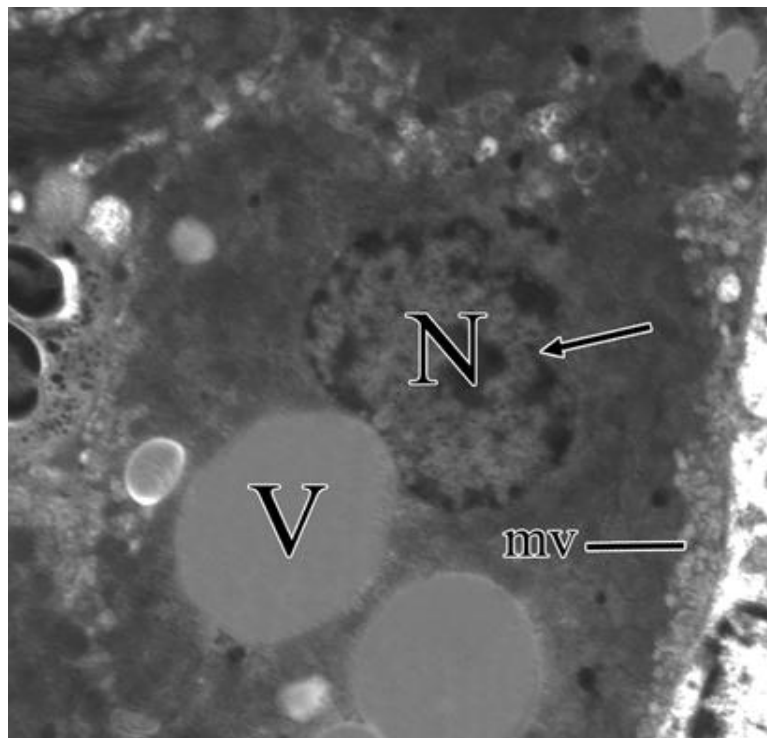


Fig. 22: an electron micrograph of a section of NaF and Ca treated rat liver (**group III**) showing an apoptotic hepatocyte exhibiting shrinkage, deformed hyperchromatic nucleus (N) with defected nuclear membrane (arrow) , high electron density of cytoplasm, large vacuoles (V) and destructed microvilli (mv). (x8000)

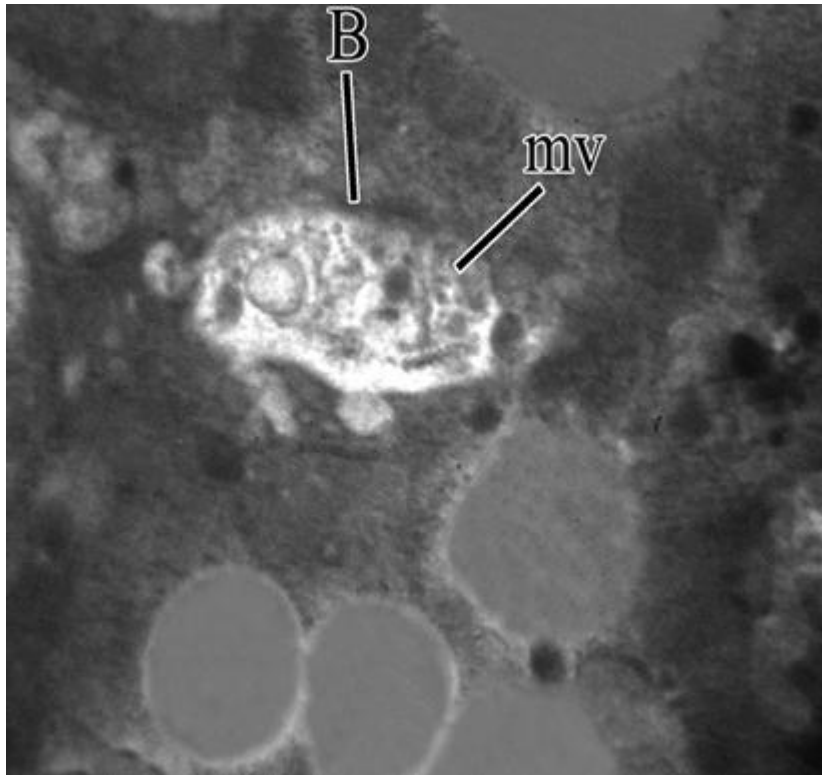


Fig. 23: an electron micrograph of a section of NaF and Ca treated rat liver (**Group III**) showing extensively dilated bile ducts(B) with severely destroyed hepatocytic microvilli (mv). (x 20000)

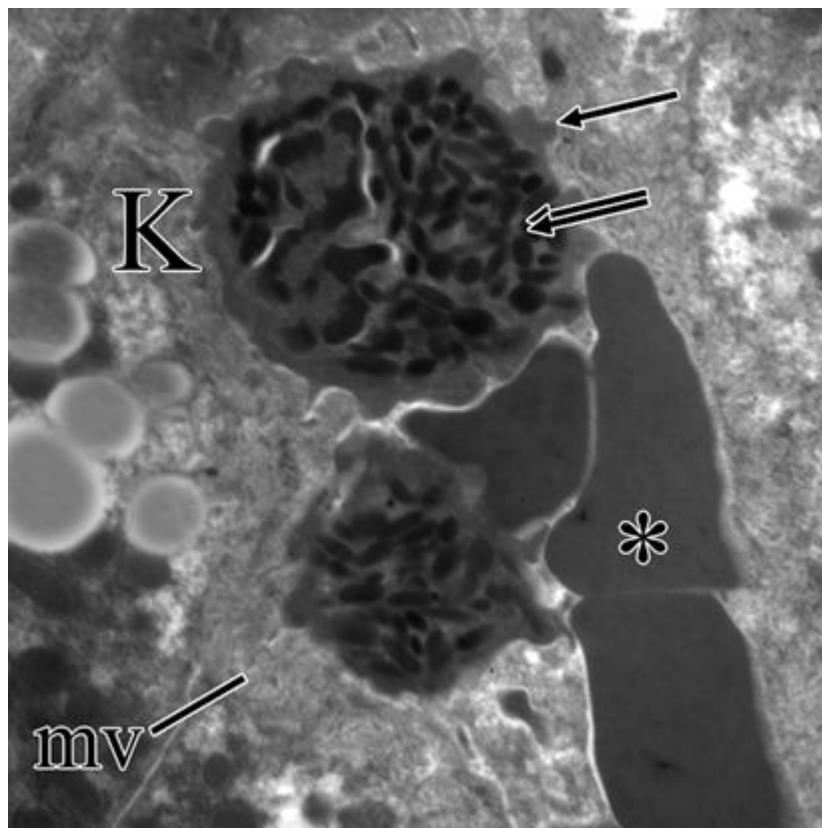


Fig. 24: an electron micrograph of a section of NaF and Ca treated rat liver (**Group III**) showing markedly dilated and congested hepatic sinusoid (*) lined with very active Kupffer cells (K) characterized by thin filipodia (arrows) and numerous phagolysosomes (arrowheads). The hepatocytic microvilli (mv) are destroyed. (x 8000)

B- Immunohistochemical and Morphometric Results:

In the present work, caspase-3 positive areas existed in the cytoplasm and cell membranes and stained brown yellow. In the control rat liver (**Group I**), Caspase 3 immunolabeled cells were rarely present (**Figure 25a**). In NaF treated rats (**Group II**), increased number of immunolabeled cells around central veins was recognized (**Figure 25 b**) suggesting increased apoptosis. In NaF and Ca treated rats (**Group III**) there was more increase in number of immunolabeled cells around the central veins if compared to other two groups (**Figure 25c**). The mean area percent analysis of the caspase-3 positive expression showed significant differences among the different groups ($p < 0.05$) as shown in **figure 26 and table 1**.

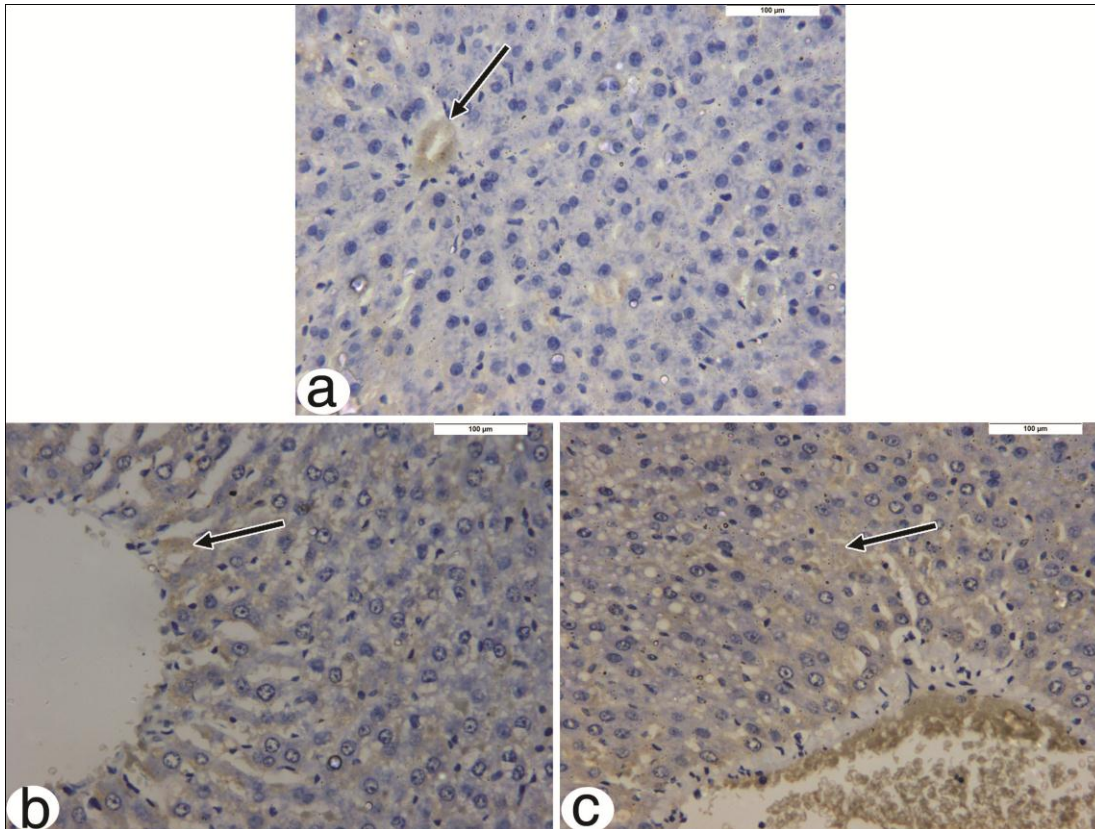


Fig.25 (a-c): photomicrographs of sections of rat liver (Caspase 3 immunostained and hematoxylin counterstained, yellow brown colour indicates immunopositivity) (x400). **(a):** control (**Group I**) showing rarely present caspase 3 immunolabeled cells (arrows). **(b):** NaF-treated (**Group II**) showing increased caspase 3 immunolabeled cells (arrows) as compared to the control group. **(c):** NaF and Ca-treated (**Group III**) showing increased caspase 3 immunolabeled cells (arrows) when compared to the other two groups.

C- Biochemical Results:

The present study showed significant differences in ALT and AST enzyme activities among the different groups ($p < 0.05$). On the other hand, there were non-significant differences ($P > 0.05$) in mean values of ALP enzyme activity among different groups of the study (**Figure 26 and table1**).

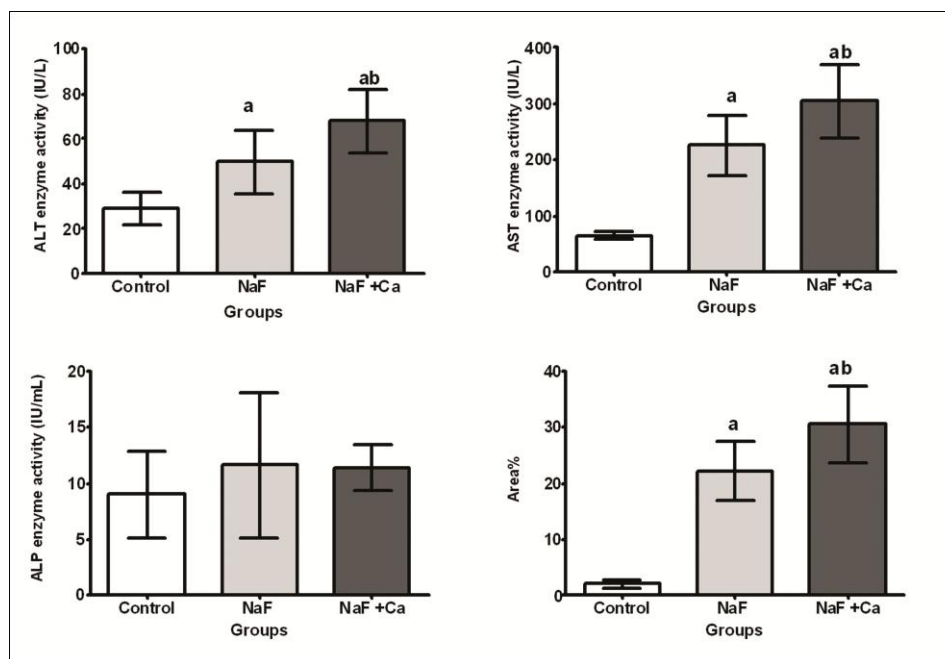


Fig. 26: showing effects of NaF alone and in combination with Ca on hepatic biomarkers (ALT, AST and ALP) and Area% of Caspase 3 expression in hepatic tissue. Values are expressed as mean \pm SD, n=6. One way ANOVA test with Post hoc Tukey's test (significant if $p \leq 0.05$), ^a significant vs control group, ^b significant vs NaF group.

Table 1: showing effects of NaF alone and in combination with Ca on hepatic biomarkers (ALT, AST and ALP) and area% of caspase 3 expression in the hepatic tissue of the different groups.

Groups			Parameter
NaF+Ca (III)	NaF (II)	Control (I)	
68 \pm 14.15 ^{ab}	49.75 \pm 13.89 ^a	29.33 \pm 7.17	ALT (IU/L)
305 \pm 65.25 ^{ab}	225.8 \pm 52.64 ^a	65.67 \pm 7.61	AST (IU/L)
11.38 \pm 1.97	11.63 \pm 6.44	9.017 \pm 3.83	ALP (IU/mL)
30.50 \pm 6.71 ^{ab}	22.29 \pm 5.29	2.07 \pm 0.72	Area%

Values are expressed as mean \pm SD, n=6. One way ANOVA test with Post hoc Tukey's test (significant if $p \leq 0.05$), ^a significant vs control group (I), ^b significant vs NaF group (II).

DISCUSSION

Compared to the control group, NaF group of the present study showed marked histopathological changes including disrupted hepatic cords, vascular dilatation and congestion, Kupffer cell proliferation and inflammatory cell infiltration. In addition, the hepatocytes exhibited vacuolization, pyknosis, necrosis and complete lysis. Similar degenerative changes have been detected by many investigators in liver tissue exposed to toxic doses of fluoride in guinea pigs⁽³¹⁾, rabbit⁽³²⁾, mice⁽³³⁾ and rats^(21, 34). Also these results are in accordance with those of rat liver exposed to drug toxicity such as 5-FU⁽³⁵⁾, cisplatin⁽³⁶⁾ and adriamycin⁽³⁷⁾.

It has been suggested that F induced vascular dilatation might be due to the direct fluoride toxicity⁽³⁸⁾. Kupffer cell hyperplasia depicted in

this work might be attributed to increased phagocytic activity of sinusoidal cells as a defense mechanism for detoxification⁽³⁹⁾ or might be a hepatic response to oxidative stress⁽⁴⁰⁾. Also, F induced inflammatory cell infiltration in the hepatic tissue was considered to result from reactive oxygen species (ROS) generation⁽⁴¹⁾. The cytoplasmic vacuolization might be a consequence to disturbed lipid and fat metabolism⁽⁴²⁾ or due to an imbalance between rates of synthesis and release of substances in hepatocytes⁽⁴³⁾. Pandey *et al.*⁽⁴⁴⁾ suggested that F induced hepatocytic necrosis might be due to glutathione depletion and oxidative stress in these cells leading to apoptotic changes followed by swelling of cell organelles especially the mitochondria and rough endoplasmic reticulum and lysosomal disintegration with subsequent necrosis, shrinkage

and nuclear dissolution of hepatocytes. In the present work, the histological alterations in liver of rats treated with fluoride are in agreement with the observed biochemical results reported in this study, where AST and ALT activities were significantly increased if compared to animals of the control group. This coincides with **Blaszczyk *et al.***⁽⁴⁵⁾ · **Yadav *et al.*** and **Jalaludeen *et al.***^(46,47) added that elevated AST and ALT activities have been used as a sensitive indicator of cytoplasmic and/or mitochondrial membrane damages.

As noted in the present results, the ultrastructural changes of hepatic cells in NaF treated group confirmed the light microscopic findings of F cytotoxicity. Furthermore, important morphological features were recognized especially structural membrane damage of mitochondria, endoplasmic reticulum, nuclear and plasma membranes. Data in this study confirmed the findings depicted by other researchers^(48,49,50,51,52,2).

It was suggested by many investigators that high F liver exposure in rat could induce lipid peroxidation with decreased antioxidative enzymatic levels and increased free radicals (ROS) generation. Subsequently, the oxidative/antioxidant balance system becomes disturbed leading to oxidative stress and oxidative damage to organs, tissues and molecules (proteins, lipids and DNA). Furthermore, DNA repair mechanisms become unable to counteract DNA damage^(53,14,21,54).

DNA damage due to ROS might explain nuclear disorganization obtained in the present study during NaF-treatment. Similar nuclear changes were detected in aluminum chloride treated mice liver⁽⁵⁵⁾.

According to the present study, in NaF treated group, the bile ducts showed manifest luminal dilatation and disruption of hepatocytes microvilli. These changes were very similar to the hepatocyte damage in aluminum-treated animals⁽⁵⁶⁾ and 5-FU treated mice⁽³⁵⁾. The previous authors attributed these changes to direct excretion of toxin or drug in bile causing bile duct damage.

The F treated animals of this work revealed significantly increased expression of caspase-3 protein and this confirms the conclusion that fluoride induces apoptosis. Similar findings have been observed in Wistar rats thymus⁽⁵⁷⁾ and fish kidney⁽⁵⁸⁾ toxicated with fluoride.

Several studies have concluded that fluoride induced apoptosis might be due to increased lipid peroxidation, oxidative stress, mitochondrial functional disturbances, downstream pathways activation and signals imbalance^(59,60,61).

Furthermore, protein activity and gene expression modification via disturbing signaling messages through multiple mechanisms might be involved in fluoride induced apoptotic cell death⁽³⁾.

This work aimed to investigate if Ca co-administration during fluoride exposure is beneficial or not against NaF induced hepatic toxicity. To our knowledge, there are no recorded reports evaluating the role of calcium on the ultrastructural NaF induced hepatic damage. As noted in these results, the structural and ultrastructural studies showed that Ca co-treatment caused more degenerative changes in liver tissue when compared to NaF treated group. These findings also explained why AST, ALT levels and area percent of caspase3 expressions showed more significant increase ($P < 0.05$) in Ca supplemented group in comparison with F treated group.

It was suggested that increased Ca^{2+} concentration might be one of the common features of cytotoxicity and cell death either directly or indirectly following changes in cellular processes⁽⁶²⁾. F and calcium relation has been suggested. Millimolar fluoride concentrations have been postulated to increase intracellular Ca^{2+} concentration in different types of cells including osteoblasts⁽⁶³⁾, erythrocytes⁽⁶⁴⁾ and renal epithelial cells⁽⁶⁵⁾ via release from intracellular Ca^{2+} stores, suppression of Ca^{2+} -pump, or activation of Ca^{2+} channels.

It has been shown that F would impair calcium homeostasis though toxic effect on mitochondria which is considered major calcium store⁽³⁾. Furthermore, the mechanism of intracellular calcium content in apoptosis induced F toxicity has been established⁽⁶⁶⁾. A direct link between the concentration of free cytosolic Ca^{2+} and the transition of cell state to apoptosis and necrosis was demonstrated in the erythrocytes of NaF treated rat⁽⁶⁴⁾. In the rat thymocytes, 10mM NaF increased an intracellular Ca^{2+} content and the population of shrunken cells⁽⁶⁷⁾. **Xu *et al.***⁽⁶⁸⁾ suggested that increased intracellular Ca^{2+} concentration might be a major role in renal tubular necrotic mechanisms in fluorosis.

In contrast, **Sun *et al.***⁽⁶⁹⁾ established that low sperm hyper activation of the mice exposed to high NaF doses was due to decrease in the cellular calcium concentration and suppression of the Ca^{2+} signaling pathway, what authors explained by the lack of endoplasmic reticulum in sperm.

Also, when F treated animals have been given Ca supplementation, F toxicity was reversed^(23,25,70,51,22). However, Ca supplementation was effective only when co

administrated with one or more of Vitamins C, D, E or with Protein.

CONCLUSION

In summary, results of this study suggested that fluoride exposure caused severe liver tissue damage. Calcium co- administration not only failed to restore hepatic damage, but also enhanced the fluoride-induced toxicity.

REFERENCES

- 1-Jha SK, Mishra VK, Sharma DK and Damodaran T (2011): Fluoride in the environment and its metabolism in humans. *Rev. Environ. Contam. Toxicol.*, 211: 121–142.
- 2-Zhang Z, Zhou B, Wang H and Xi S (2014): Maize purple plant pigment protects against fluoride-induced oxidative damage of liver and kidney in rats. *International Journal of Environmental Research and Public Health*, 11:1020–1033.
- 3- Barbier O, Arreola-Mendoza L and Del Razo LM (2010): Molecular mechanisms of fluoride toxicity. *Chem. Biol. Interact.*, 188:319–333.
- 4-Lech T (2011): Fatal cases of acute suicidal sodium and accidental zinc fluorosilicate poisoning. Review of acute intoxications due to fluoride compounds. *Forensic. Sci. Int.*, 206: 20–24.
- 5-Zhou T, Duan LJ, Ding Z, Yang R P, Li SH, Xi Y, Cheng X, Hou J, Wen S, Chen J, Cui L and Ba Y (2012): Environmental fluoride exposure and reproductive hormones in male living in endemic fluorosis villages in China. *Life Science Journal*, 9 (4):1-7.
- 6-Fawell J, Bailey K, Chilton J, Dahi E, Fewtrell L and Magara Y (2006): WHO, Fluoride in Drinking Water. IWA Publishing Company, London, UK.
- 7-Shashi A, Singh JP and Thapar SP (2002): Toxic effects of fluoride on rabbit kidney. *Fluoride*, 35: 38-50.
- 8-Shashi A (2003): Histopathological investigation of fluoride-induced neurotoxicity in rabbits. *Fluoride*, 36: 95–105.
- 9-Karadeniz A and Altıntas L (2008): Effects of Panax Ginseng on fluoride-induced haematological pattern changes in mice. *Fluoride*, 41: 67–71.
- 10- Lu Y, Luo Q, Cui H, Deng H, Kuang P, Liu H, Fang J, Zuo Z, Deng J, Li Y, Wang X and Zhao L (2017): Sodium fluoride causes oxidative stress and apoptosis in the mouse liver. *Aging*, 9(6):1623-1639.
- 11- Deng H, Kuang P, Cui H, Chen L, Luo Q and Zhao L (2016): Sodium fluoride (NaF) induces the splenic apoptosis via endoplasmic reticulum (ER) stress pathway *in vivo* and *in vitro*. *Aging*, 8:3552–3567.
- 12- Kuang P, Deng H, Cui H, Chen L, Fang J, Zuo Z, Deng J, Wang X and Zhao L (2017): Sodium fluoride (NaF) causes toxic effects on splenic development in mice. *Oncotarget.*, 8:4703–4717.
- 13- Luo Q, Cui H, Deng H, Kuang P, Liu H, Lu Y and Zhao L (2017): Histopathological findings of renal tissue induced by oxidative stress due to different concentrations of fluoride. *Oncotarget.*, 8(13):50430-50446.
- 14-Nabavi SF, Nabavi SM, Habtemariam S, Moghaddam AH, Sureda A, Jafari M and Latifi AM (2013): Hepatoprotective effect of gallic acid isolated from *Peltiphyllum peltatum* against sodium fluoride-induced oxidative stress in rat's kidney. *Molecular and Cellular Biochemistry*, 372:233–239.
- 15-Malarvizhi A, Kavitha C, Saravanan M and Ramesh M (2012): Carbamazepine (CBZ) induced enzymatic stress in gill, liver and muscle of a common carp, *Cyprinus carpio*. *J. King Saud Univ. Sci.*, 24:179-186.
- 16- Zhou BH, Zhao J, Liu J, Zhang JL, Li J and Wang HW (2015): Fluoride induced oxidative stress is involved in the morphological damage and dysfunction of liver in female mice. *Chemosphere*, 139:504–511.
- 17- Song, G.H., Huang, F.B., Gao, J.P. Liu ML, Pang WB, Li WB, Yan XY, Huo MG and Yang X (2015): Effects of fluoride on DNA damage and Caspase-mediated apoptosis in the liver of rats. *Biol. Trace Elem. Res.*, 166(2):173–182.
- 18- Agha FE, El-Badry MO, Hassan D and Elraouf A A (2012): Role of vitamin E combination with methionine and L-carnosine against sodium fluoride-induced hematological, biochemical, DNA damage, histological and immunohisto-chemical changes in pancreas of albino rats. *Life Sci. J.*, 9: 1260–1275.
- 19-Nabavi SM, Nabavi SF, Eslami S and Moghaddam AH (2012): *In vivo* protective effects of quercetin against sodium fluoride-induced oxidative stress in the hepatic tissue. *Food Chem.*, 132: 931–935.
- 20-Trivedi MH, Verma RJ, Sangai NP and Chinoy NJ (2012): Mitigation by black tea extract of sodium fluoride-induced histopathological changes in brain of mice. *Fluoride*, 45: 13–26.
- 21- Panneerselvam L, Subbiah K, Arumugam A and Senapathy JG (2013): Ferulic acid modulates fluoride-induced oxidative hepato-toxicity in male Wistar rats. *Biol. Trace Elem. Res.*, 151: 85–91.
- 22-Mohamed NE (2014): The Role of Calcium in Ameliorating the Oxidative Stress of Fluoride in Rats. *Research and Reviews: Journal of Zoological Sciences (RRJZS)*, 2 (3): 6-19.
- 23-Chinoy NJ and Sharma A (2000): Reversal of fluoride-induced alteration in cauda epididymal spermatozoa and fertility impairment in male mice. *Environmental Sciences*, 7(1):29-38.
- 24-Ba Y, Zhu JY, Yang YJ, Yu B, Huang H, Wang G, Ren LJ, Cheng XM, Cui, LX and Zhang YW (2010): Serum calciotropic hormone levels and dental fluorosis in children exposed to different concentrations of fluoride and iodine in drinking water. *Chin. Med. J.*, 123: 675–679.

- 25-Das SS, Maiti R and Ghosha D (2006):** Management of fluoride induced testicular disorder by calcium and vitamin E co-administration in the albino rat. *Reprod. Toxicol.*, 22: 606-612.
- 26-Guney M, Oral B, Karahan N and Mungana T(2007):** Protective effect of caffeic acid phenethyl ester (CAPE) on fluoride-induced oxidative stress and apoptosis in rat endometrium. *Environmental Toxicology and Pharmacology*, 24:86–91.
- 27-Reitman S and Frankel S (1957):** A colorimetric method for the determination of serum glutamic oxaloacetic acid and glutamic pyruvic transaminases. *Am. J. Clin. Pathol.*, 28: 56-63.
- 28-Suvarna SK, Layton C, Bancfort JD and Stevens A (2013):** Theory and Practice of Histological Techniques, 7th ed., Churchill Livingstone, London,USA.
- 29-Glauert A M and Lewis P R (1999):** Biological specimen preparation for transmission electron microscopy. *Parasitology Today*, 15(9):392-399.
- 30-Unger CA, Buchmann CL, Bunemann SK and Schwarz M (1998):** Wild-type function of the p53 tumor suppressor protein is not required for apoptosis of mouse hepatoma cells. *Cell Death Differ.*, 5:87–95.
- 31-Kour K, Koul ML and Koul RL (1981):** Histological changes in liver following sodium fluoride ingestion. *Fluoride*, 14(3):119- 123.
- 32-Shashi A and Thapar SP (2001):** Histopathology of fluoride-induced hepatotoxicity in rabbits. *Fluoride*, 34 (1): 34-42.
- 33-Lu J, Zheng J, Liu H, Li J, Xu Q and Chen K (2010):** Proteomics analysis of liversamples from puffer fish Takifugu rubripes exposed to excessive fluoride: aninsight into molecular response to fluorosis. *J. Biochem. Mol. Toxicol.*, 24: 21–28.
- 34-Parihar S, Choudhary A, and Gaur, S. (2013):** Toxicity of fluoride in liver of Albino rat and Mitigation after adopting artificial (Vitamin C and D) and natural (Aloe vera) food supplementations. *International Journal of Advancements in Research and Technology*, 2 (2): 1-11
- 35-Abou-Zeid NR (2014):** Ameliorative effect of vitamin C against 5-fluorouracil-induced hepatotoxicity in mice: a light and electron microscope study. *The Journal of Basic and Applied Zoology*, 67:109–118.
- 36-Cetin A, Arslanbas U, Saraymen B, Canoz O, Ozturk A and Sagdic O (2011):** Effects of grape seed extract and *Origanum onites* essential oil on cisplatin-induced hepatotoxicity in rats. *Int. J. Hematol. Oncol.*, 21 (3):133–139.
- 37-Sakr SA, Mahran HA and Lamfon HA (2011):** Protective effect of ginger (*Zingiber officinale*) on adriamycin induced hepatotoxicity in albino rats. *J. Med. Plant Res.*, 5 (1):133–140.
- 38-Klatskin G and Ocean HO (1993):** In: *Histopathology of the Liver*, Vol.1. Oxford University Press, Oxford and New York.
- 39-Nehru B and Kaushal S (1993):** Alterations in the hepatic enzymes following experimental lead poisoning. *Biol. Trace Elem. Res.*, 38: 27–34.
- 40-Neyrinck A (2004):** Modulation of Kupffer cell activity: physio-pathological consequences on hepatic metabolism. *Bull. Mem. Acad. R. Med. Belg.*, 159 : 358–366.
- 41-Johar D, Roth JC, Bay GH, Walker JN, Krocak TJ and Los M (2004):** Inflammatory response, reactive oxygen species, programmed (necrotic-like and apoptotic) cell death and cancer. *Rocz. Akad. Med. Bialymst.*, 49: 31–39.
- 42-Zhang LY and Wang CX (1984):** Histopathological and histo-chemical studies on toxic effect of brodifacoum in mouse liver. *Acta Acad. Med. Sci.*, 6 (5):386–388.
- 43-Blankenship LJ, Manning FC, Orenstin JM and Patierno SR (1994):** Apoptosis is the mode of cell death caused by carcinogenic chromium. *Toxicol. Appl. Pharmacol.*, 126:75-83.
- 44-Pandey G, Srivastava DN and Madhuri S (2008):** A standard hepatotoxic model produced by paracetamol in rat. *Toxicol. Int.*, 15 (1): 69–70.
- 45-Blaszczyk I, Birkner E, Kasperczyk S (2011):** Influence of methionine on toxicity of fluoride in the liver of rats. *Biol. Trace Elem. Res.*, 139:325-331.
- 46-Yadav SS, Kumar R and Tripathi M (2014):** Effects of fluoride exposure on some enzymatic and histopathological changes in the liver of *Heteropneustes fossilis* (Bloch). *International Journal of Fauna and Biological Studies*, 1 (5): 80-84.
- 47-Jalaludeen AM, Ha WT, Lee R, Kim JH, Do JT, Park C, Heo YT, Lee WY and Song H(2016):** Biochanin A ameliorates arsenic-induced hepato and hematotoxicity in rats. *Molecules*, 21(1): 69-75.
- 48- Dabrowska E, Balunowska M, Letko R and Szynaka, B (2004):** Ultrastructural study of the mitochondria in the submandibular gland, the pancreas and the liver of young rats, exposed to NaF in drinking water. *Rocz. Akad. Med. Bialymst.*, 49 (1): 180-181.
- 49-Dabrowska E, Letko R and Baluno-wska M (2006):** Effect of sodium fluoride on the morphological picture of the rat liver exposed to NaF in drinking water. *Adv. Med. Sci.*, 51 (1): 91-95.
- 50-Chattoadhyay A, Podder S, Agarwal S and Bhattacharya S (2011):** Fluoride-induced histopathology and synthesis of stress protein in liver and kidney of mice. *Arch. Toxicol.*, 85:327-335.
- 51-Liang Z, Niu R, Wang J, Wang H, Sun Z and Wang J (2012):** Ameliorative effect of protein and calcium on fluoride induced hepatotoxicity in rabbits. *Afr. J. Biotechnol.*, 11(73): 13801-13808.
- 52-Cao J, Chen J, Wang J, Jia R, Xue W, Luo Y and Gan X (2013):** Effects of fluoride on liver apoptosis and Bcl2, Bax protein expression in freshwater teleost, *Cyprinus carpio*. *Chemosphere*, 91:1203–1212.

- 53-Hassan HA and Abdel-Aziz AF (2010):** Evaluation of free radical scavenging and antioxidant properties of black berry against fluoride toxicity in rats. *Food Chem. Toxicol.*, 48:1999–2004.
- 54-Atmaca N, Atmaca HT, Kanici A and Anteplioglu T(2014):** Protective effect of resveratrol on sodium fluoride-induced oxidative stress, hepatotoxicity and neurotoxicity in rats. *Food Chem. Toxicol.*, 70: 191–197.
- 55-El-Sayed W M, Al-Kahtani MA and Abdel-Moneim AM (2011):** Prophylactic and therapeutic effects of taurine against aluminum-induced acute hepato-toxicity in mice. *Journal of Hazardous Materials*, 192: 880– 886.
- 56-Alemmari A, Miller GG, Arnold, CG and Zello, GA (2011):** Parenteral aluminum induces liver injury in a newborn piglet model. *Journal of Pediatric Surgery*, 46: 883–887.
- 57-Ren G, Ferreri M, Wang Z, Su Y, Han B and Su J(2011):** Sodium fluoride affects proliferation and apoptosis through insulin-like growth factor I receptor in primary cultured mouse osteoblasts. *Biol. Trace Elem. Res.*, 144(1-3):914–923.
- 58-Chen J, Cao J, Wang J, Jia R, Xue W, Zie L (2015):** Fluoride-induced apoptosis and expressions of caspase proteins in the kidney of carp (*Cyprinus carpio*). *Environmental Toxicology*, 30(7):769-781.
- 59-Flora SJ, Mittal M and Mishra D (2009):**Co-exposure to arsenic and fluoride on oxidative stress, glutathione linked enzymes, biogenic amines and DNA damage in mouse brain. *J. Neurol. Sci.*, 285:198–205.
- 60-Karuber H, Nishitai G, Inageda K, Kurosu H and Matsuoka M (2009):** NaF activates MAPKs and induces apoptosis in odontoblast-like cells. *J. Dent. Res.*, 88:461–465.
- 61-Mohammadi S, Movahedin M and Mowla SJ (2009):** Up-regulation of CatSper genes family by selenium. *Reprod. Biol. Endocrino.*, 7: 126-133.
- 62-Berridge MJ, Lipp P and Bootman MD (2000):** The versatility and universality of calcium signalling. *Nature Reviews Molecular Cell Biology*, 1 (1): 11–21.
- 63-Zerwekh JE, Morris AC, Padalino PK, Gottschalk F and Pak, CY C. (1990):** Fluoride rapidly and transiently raises intracellular calcium in human osteoblasts. *Journal of Bone and Mineral Research*, 5(1): 131–136.
- 64-Agalakova N I and Gusev G P (2011):** Fluoride-induced death of rat erythrocytes *in vitro*. *Toxicology in Vitro*, 25(8):1609–1618.
- 65-Murao H , Sakagami N, Iguchi T , Murakami T and Suketa Y (2000):** Sodium fluoride increases intracellular calcium in rat renal epithelial cell line NRK-52E. *Biological and Pharmaceutical Bulletin*, 23(5): 581–584.
- 66-Kubota K, Lee DH, Tsuchiya, M, Young, CS, Everett ET, Martinez-Mier EA, Snead ML, Nguyen L, Urano F and Bartlett JD (2005):** Fluoride induces endoplasmic reticulum stress in ameloblasts responsible for dental enamel formation. *J. Biol. Chem.*, 280: 23194–23202.
- 67-Matsui H, Morimoto M, Horimoto K and Nishimura Y (2007):** Some characteristics of fluoride-induced cell death in rat thymocytes: cytotoxicity of sodium fluoride. *Toxicology in Vitro*, 21 (6):1113–1120.
- 68- Xu H, Zhou YL, Zhang JM, Liu H, Jing L and Li GS (2007):** Effects of fluoride on the intracellular free Ca²⁺ and Ca²⁺-ATPase of kidney . *Biological Trace Elements*, 116 (3): 279-287.
- 69-Sun Z, Niu R, Su K, Wang B, Wang J, Zhang J and Wang J (2010):** Effects of sodium fluoride on hyperactivation and Ca²⁺ signaling pathway in sperm from mice: an *in vivo* study. *Archives of Toxicology*, 84 (5): 353–361.
- 70-Sarkar, SD. (2006):** Management of fluoride induced testicular disorders by calcium and vitamin-E co-administration in the albino rat. *Reprod. Toxicol.*, 22(4):606-612.